Available online at www.sciencedirect.com
SCIENCE DIRECT
Polymer 47 (2006) 5831–5837
polymer
www.elsevier.com/locate/polymer

PAN/SAN/SWNT ternary composite: Pore size control and electrochemical supercapacitor behavior

Chongfu Zhou, Tao Liu[1], Tong Wang, Satish Kumar*

School of Polymer, Textile and Fiber Engineering, Georgia Institute of Technology, P.O. Box 0295, 801 Ferst Dr., Atlanta, GA 30332, USA

Received 6 April 2006; received in revised form 27 May 2006; accepted 1 June 2006
Available online 30 June 2006

Abstract

Single wall carbon nanotubes (SWNT) act as a compatabilizer for polyacrylonitrile (PAN)/styrene–acrylonitrile (SAN) copolymer blends. Carbonization of PAN/SAN/SWNT blend films results in pore widths in the range of 1–200 nm, while carbonized PAN/SAN blend films resulted in pores with typical width of 1–10 μm. Electrochemical supercapacitor behavior of the carbonized PAN/SAN/SWNT films was characterized using 6 M KOH electrolyte. Surface area and pore size distribution were analyzed using nitrogen gas adsorption and the BET and DFT theories. Double layer capacity of the carbonized PAN/SAN/SWNT films was as high as 205 μF/cm^2 based on the BET surface area.

Keywords: Carbon nanotube; Supercapacitor; Polyacrylonitrile

1. Introduction

Pore size control in carbon materials is important for many applications including electrochemical supercapacitors [1–4], catalysis [5,6], and filtration [7]. Activation is a common method for achieving porous carbons with high surface area [8–10]. Other methods for producing porous carbon include emulsification [11,12], aerogel–xerogel formation [13], phase separation [14], phase inversion [15], and silica sol–gel templates [16–18]. Carbonization of triblock copolymers (ABA) such as acrylonitrile (A) and *n*-butyl acrylate (B) has also been reported to provide nanosize porosity control in carbon [19]. Polyacrylonitrile (PAN) is a carbonizing polymer. Carbonized and activated polyacrylonitrile [20] as well as polyacrylonitrile/carbon nanotube composites [26] have been used for electrochemical supercapacitors. Polypyrrole covered carbon nanotubes have also been used for supercapacitor electrodes [21–23]. Styrene–acrylonitrile (SAN) copolymer is a polymer that completely burns out when heated above 600 °C either in air or in inert environment and can therefore be used for pore size control. SAN is immiscible in PAN [28]. In this study it has been shown that in the presence of single wall carbon nanotubes, SAN can be dispersed in PAN matrix and can be used for pore size control. Surface area, pore size distribution, and electrochemical supercapacitor behavior of carbonized PAN/SAN/SWNT blend films have been reported in this paper.

2. Experimental

Solution of PAN (containing less than 5% itaconic acid and methacrylate copolymer, from Enichem Solution Corp) and SAN (25 wt% acrylonitrile and 75 wt% styrene random copolymer, Mw = 165,000 g/mol, from ACROS Organics) in dimethylformamide (DMF, obtained from Fisher Scientific and used as received) was prepared in the desired PAN:SAN ratio in 40 g DMF. To this solution, unpurified HiPCO single wall carbon nanotubes (35 wt% or about 7 at% catalytic impurity (Fe) [24], from Carbon Nanotechnologies, Inc.) were added to make a PAN/SAN/SWNT suspension with total solid content of 150 mg. In the preparation of suspension, a few

* Corresponding author. Tel.: +1 404 894 7550.
E-mail addresses: liutao@battelle.org (T. Liu), satish.kumar@gatech.edu (S. Kumar).
[1] Current address: Battelle Memorial Institute, 505 King Avenue, Columbus, OH 43201, USA.

0032-3861/$ - see front matter © 2006 Elsevier Ltd. All rights reserved.
doi:10.1016/j.polymer.2006.06.003

Table 1
Compositions of PAN/SAN/SWNT composite films

	PAN1				PAN2	PAN3
	SAN0	SAN10	SAN30	SAN50	SAN30	SAN30
SAN (%)	0	10	30	50	30	30
SWNT (%)	10.2	9.2	7.1	5.1	3.4	11.4
PAN (%)	89.8	80.8	62.9	44.9	66.6	58.6
PAN:SWNT	9:1	9:1	9:1	9:1	20:1	5:1
Residual weight on carbonization (%)	69.7	61.5	48.5	36.1	45.4	50.2

minutes of homogenization (Biohomogenizer M133/1281-0, ESGE, Switzerland) followed by 30 min of sonication (Ultrasonic processor, 550 W, 20 kHz, Misonix Inc.) was applied. The PAN/SAN/SWNT films were cast on a glass substrate by DMF evaporation in vacuum at 85 °C. The film thickness before carbonization was about 25 μm. Various PAN/SAN/SWNT compositions used in this study are listed in Table 1. For the PAN1 series films, PAN:SWNT weight ratio is constant at 9:1, while SAN concentration is varied from 0 to 50 wt%. For PAN2 and PAN3 series films, the PAN:SWNT weight ratios are 20:1 and 5:1, respectively, while SAN concentration is constant at 30 wt%.

The composite films were stabilized in a box furnace (Lindberg, 51668-HR Box Furnace 1200C, Blue M Electric) at 250 °C in air for 2 h and carbonized in argon at 700 °C for 30 min. Thermogravimetric analysis of the SAN copolymer was carried out in TGA 2950 (TA Instruments, Inc.) by heating the sample in air (or in nitrogen) at 5 °C/min. The SEM observation was done on gold-coated samples on LEO 1530. The isothermal N_2 gas adsorption was carried out on ASAP 2020 (Micromeritics Inc.) at 77 K. For gas adsorption study, samples were degassed at 90 °C for 16 h at a pressure of 10^{-4} Pa, and the data analysis was done using BET and DFT [25] methods. Mass of the sample after-degassing was used for the determination of the specific surface area. X-ray photoelectron spectroscopy (XPS) results were obtained on SSX-100

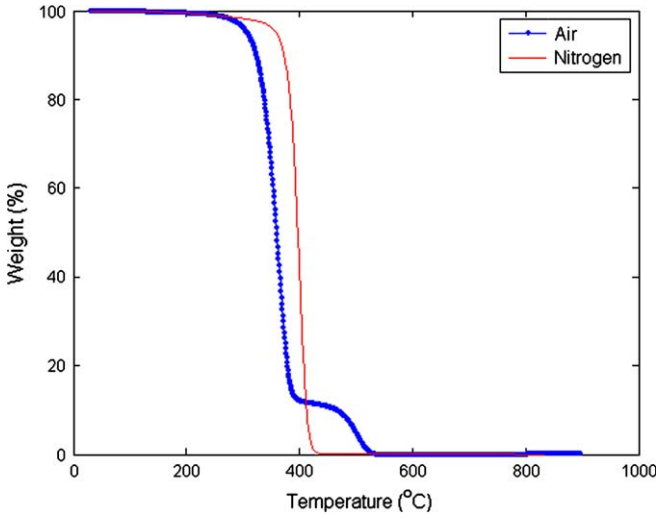

Fig. 1. Thermogravimetric analysis of SAN in air and in nitrogen at a heating rate of 5 °C/min.

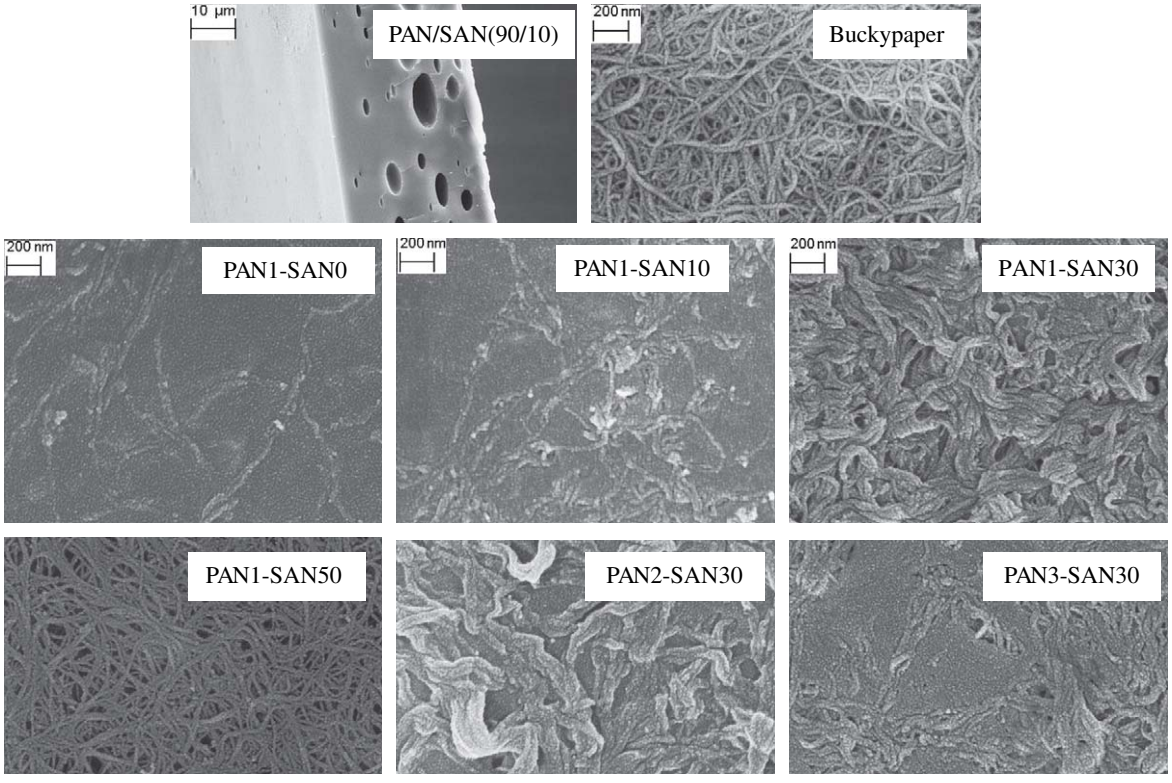

Fig. 2. Scanning electron micrographs of carbonized PAN/SAN (90/10) film, SWNT bucky paper, and carbonized PAN/SAN/SWNT films. Compositions of carbonized PAN/SAN/SWNT films are listed in Table 1.

ESCAE Spectrometer using Al Kα radiation ($h\nu = 1486.6$ eV) operated at 10 kV. The vacuum in the analysis chamber was about 5×10^{-9} Torr. The spectra analysis was accomplished using ESCA 2000.

Constant current (CC, 0.5–5 mA) charging–discharging and cyclic voltammetry (CV, 5–200 mV/s) measurements were carried out on Solartron 1470 at room temperature, using two film electrodes (diameter = 1.27 cm) separated by Celgard 3400 microporous membrane and sandwiched between nickel current collectors. KOH aqueous solution (6 M) was used for capacitance evaluation between 0 and 0.8 V. Comparable results were obtained from the CC and CV studies. The specific capacitance (C_{sp}) was calculated using the previously reported method [26].

3. Results and discussion

Thermogravimetric analysis shows that SAN leaves no residue when heated to 700 °C in air or in N_2 (Fig. 1) and is the basis of the pore size control. The compositions of various PAN/SAN/SWNT ternary composite samples along with the residual weight of the films carbonized at 700 °C are listed in Table 1. The residual weight data are consistent with the complete SAN burn out. Scanning electron micrographs of a carbonized PAN/SAN film without SWNT, SWNT bucky paper [27] and carbonized PAN/SAN/SWNT films are given in Fig. 2. Carbonized PAN/SAN film without SWNT exhibits pores with typical dimensions in the 1–10 μm range. This is a result of SAN domains which have been burned out on carbonization. The SAN domain size is consistent with the literature reports on PAN/SAN phase behavior [28]. By comparison, the pore width in carbonized PAN/SAN/SWNT films as quantified by the nitrogen gas adsorption analysis (Fig. 3) is much smaller than that in PAN/SAN films (Fig. 2a). The average pore size in the SWNT bucky paper was 5.6 nm with a total pore volume of 0.76 cm^3/g, and the average pore size in the various PAN/SAN/SWNT samples ranged from 3 to 13 nm (Table 2). The sample containing no SAN, exhibited negligible pore volume (0.01 cm^3/g) and pore volume increased to 0.28 cm^3/g with increasing SAN and SWNT contents. Data in Table 2 also show that at a given PAN:SWNT ratio (9:1), surface area and pore volume increased with SAN content. Variation in PAN:SWNT ratio (20:1, 9:1, and 5:1), at a given SAN content (30%) did not result in significant change in the average pore size (11 and 13 nm), while the total pore volume and the surface area did increase with increasing SWNT content (Table 2). This study shows that the presence of SWNT serves to act as a compatabilizer for PAN/SAN blends. In PAN/SAN blends, SAN phase separates due to the immiscibility of styrenic and nitrile moieties. There is good interaction between PAN and SWNT [29,30]. The fact that SAN is homogeneously dispersed in PAN matrix in the presence of SWNT suggests that SWNT–styrene and SWNT–nitrile interactions are fairly comparable, leading to SWNT compatabilizer behavior. The polymer blend morphology in the presence of single wall carbon nanotubes remains unexplored,

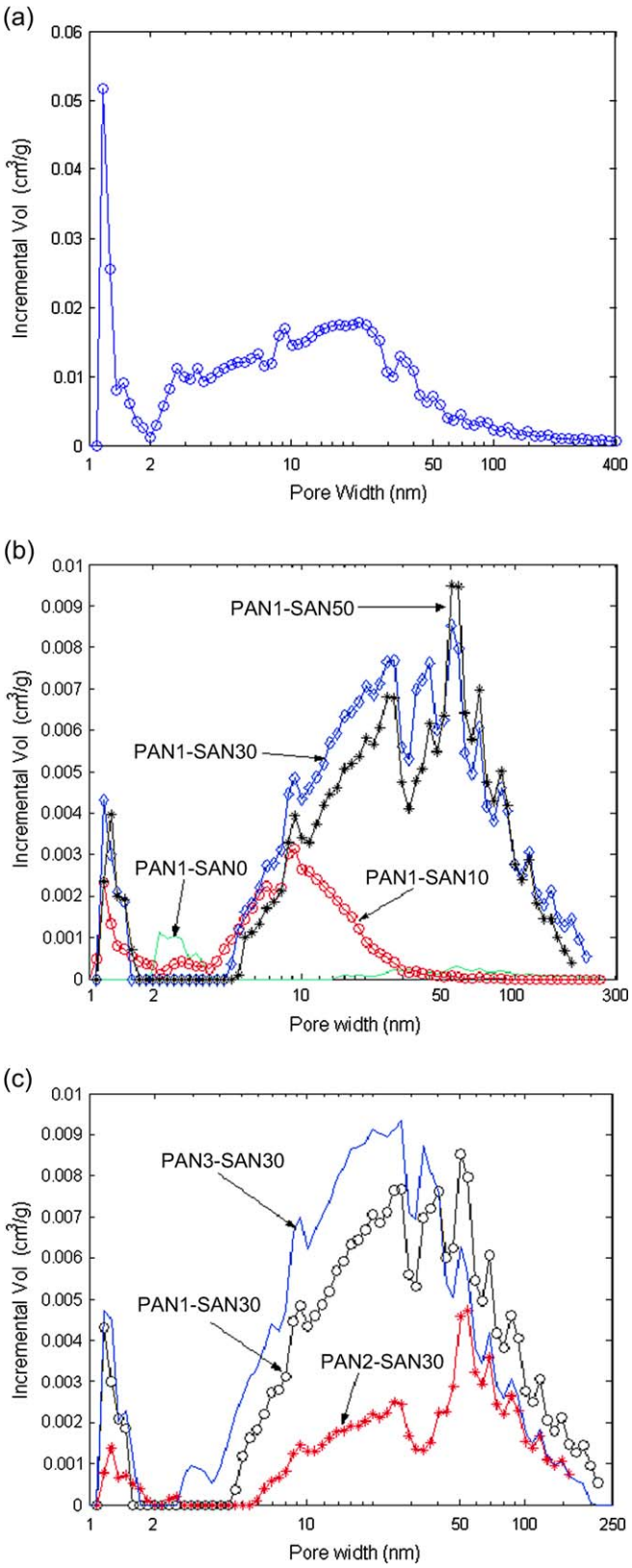

Fig. 3. Pore size distribution in (a) SWNT bucky paper, (b) and (c) carbonized PAN/SAN/SWNT films. Compositions of carbonized PAN/SAN/SWNT films are listed in Table 1.

Table 2
Specific capacitance, surface area, pore volume and double layer capacity of SWNT bucky paper and carbonized PAN/SAN/SWNT composites

	PAN1				PAN2	PAN3	SWNT bucky paper
	SAN0	SAN10	SAN30	SAN50	SAN30	SAN30	
Capacitance (F/g) at 0.1 V	11 ± 1	96 ± 1.2	106 ± 0.7	114 ± 1.2	78 ± 1.3	110 ± 0.4	55 ± 0.1
Capacitance (F/g) at 0.4 V	10 ± 0.3	85 ± 0.7	84 ± 0.2	72 ± 0.3	54 ± 0.4	89 ± 0.2	49 ± 0.1
Capacitance (F/g) at 0.7 V	5 ± 0.5	65 ± 1.6	62 ± 1.1	39 ± 0.4	29 ± 0.3	74 ± 0.3	41 ± 0.1
BET surface area (m^2/g)	16	50	87	115	38	132	546
DFT surface area (m^2/g)	5	23	48	60	21	70	297
DFT pore volume (cm^3/g)	0.01	0.06	0.24	0.22	0.09	0.28	0.72
Average pore width (nm)	3	5	13	11	13	11	5.6
C_{dl} (μF/cm^2)							
BET	69	192	122	99	205	83	10
DFT	220	417	221	190	371	157	19

and to the best of our knowledge this is the first report on a topic that promises to be quite rewarding with many different polymer combinations. Pyrolysis of SAN domains, which are formed by the phase separation of the SAN from the PAN matrix due to the immiscibility of the styrene segments, is responsible for the observed porous structure.

Charging–discharging voltage as a function of time (constant current measurement, CC) and specific capacitance as

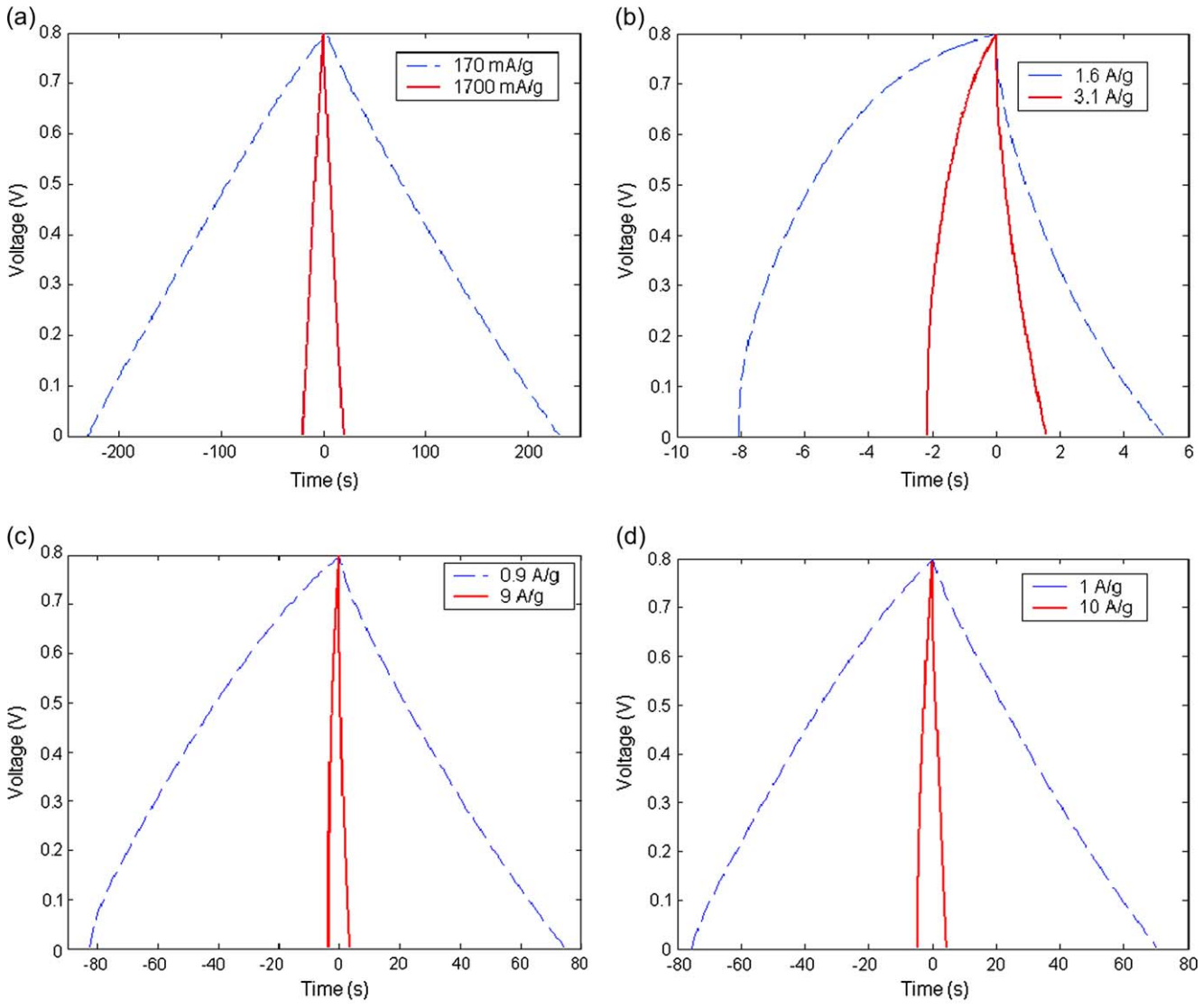

Fig. 4. Constant current charging–discharging behavior of different samples at two current densities. (a) Bucky paper, (b) PAN1–SAN0, (c) PAN1–SAN30, and (d) PAN3–SAN30.

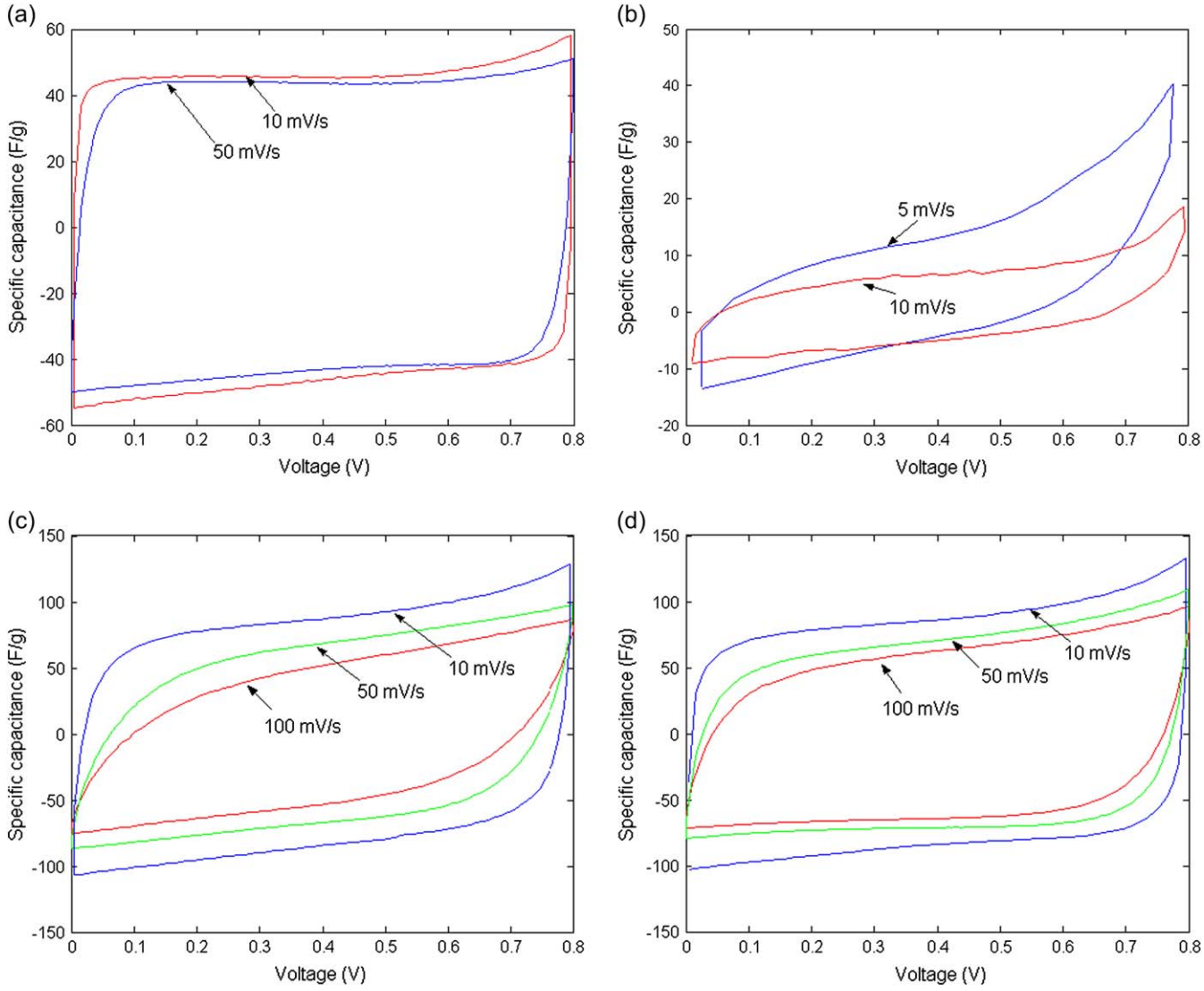

Fig. 5. Cyclic voltammograms at different scan rates for various samples. (a) Bucky paper, (b) PAN1–SAN0, (c) PAN1–SAN30, and (d) PAN3–SAN30.

a function of voltage (cyclic voltammetry measurement, CV) for selected samples are shown in Figs. 4 and 5, respectively. CC and CV are routine supercapacitor test methods [15]. In CC measurements, the test cell is subjected to a cyclic square-wave current, and the voltage response is measured as a function of time, which commonly shows the saw-tooth like shape as observed in Fig. 4. In CV measurements, voltage sweep with saw-tooth shape wave is applied to the test cell, and the current response is recorded, which is typically a rectangular or parallelogram shape as observed in Fig. 5. Based on the CC and CV test results, the specific capacitance (C_{sp}) of various carbonized PAN/SAN/SWNT films is calculated using the previously reported method [26]. Current density as a function of scan rate (at 0.1 V) from CV measurement is plotted in Fig. 6. All three figures show that the behavior of PAN1–SAN0 deviates significantly from linearity, suggesting a distributive capacitance behavior. Fig. 6 also shows that PAN1–SAN30 as well as PAN2–SAN30 also deviates from linearity moderately. This may arise from surface functional groups inducing pseudocapacitance as well as a broad pore size distribution. However, considering the complex electrochemical response of porous materials, it is difficult to unambiguously separate the capacitance contribution from each factor individually [15].

The samples containing SAN copolymer have significantly higher capacitance than the samples without SAN (Table 2). The errors reported for the supercapacitor values in Table 2 and for current density in Fig. 6 are based on CC or CV measurements for 6 consecutive cycles. Capacitance performance does deteriorate when samples are tested over large number of charge–discharge cycles. For example, after 10,000 charge–discharge cycles in 6 M KOH, the capacitance of PAN3–SAN30 sample decreased to about 25% of its original value. Significantly larger errors (up to 30%) were observed when samples carbonized in a different batch were tested. Specific capacitance of the bucky paper, a 100% SWNT film, was in the range of 41–55 F/g, consistent with the literature reports [26,31,32,23]. Surface area of the bucky paper is significantly

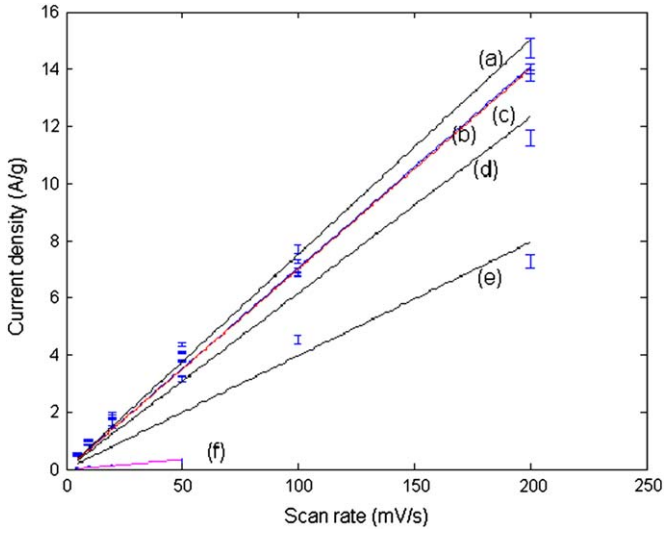

Fig. 6. Current density as a function of scan rate for various samples. (a) PAN1–SAN50, $R^2 = 0.995$; (b) PAN3–SAN30, $R^2 = 0.998$; (c) PAN1–SAN10, $R^2 = 0.995$; (d) PAN1–SAN30, $R^2 = 0.969$; (e) PAN2–SAN30, $R^2 = 0.916$; and (f) PAN1–SAN0, $R^2 = 0.901$. R^2 is the correlation coefficient. Low R^2 value indicates significant deviation from linear behavior.

higher than the surface area of any of the composite film, however, the bucky paper is dominated by micropores (Fig. 3a). Most micropores are not accessible to the electrolytes, and therefore do not contribute to the capacitance. The double layer capacity of the bucky paper is consistent with the double layer capacity of graphite and activated carbons, which are reported to be in the range of 3–70 μF/cm^2 [1,15]. Double layer capacity of the recently reported carbonized PAN/MWNT composites was in the range of 24–64 μF/cm^2 [33]. The double layer capacity of various PAN/SAN/SWNT ternary composite samples are in the range of 83–205 μF/cm^2 calculated based on the BET surface area and much higher when calculated based on the DFT surface areas (Table 2). This may in part be attributed to pseudocapacitance as well as a high percentage of the total surface area being accessible to the electrolyte for charge storage.

Carbonized composite films were analyzed using XPS, and their carbon, nitrogen and oxygen contents are listed in Table 3. Under these carbonization conditions, all composite samples typically contain 3–5 wt% nitrogen and 6–15 wt% oxygen. Significant amounts of oxygen and nitrogen in the composite films can also be seen by resolving C1s peak into 3 individual peaks [34,35], which are C–C at 284.8 eV, C–O (phenolic, ether) and C–N at 285.8 eV, and C=O (carbonyl or quinone) at 287.2 eV. The concentrations of C–C, C–O (C–N), and C=O groups in these carbonized PAN/SWNT/SAN samples were in the range of 67–78%, 17–24%, and 5–9%, respectively. Pyridinic nitrogen [33], as well as oxygen-containing functional groups may contribute to the pseudocapacitance behavior. As compared to SWNT bucky paper, all composite films exhibit significantly reduced microporosity (pores < 2 nm, Fig. 3). The contribution of the pseudocapacitance for the samples exhibiting linear behavior in Fig. 6, is not likely to be very high. The high double layer capacity in these films, at least in part can be attributed to the reduced microporosity.

Table 3
Composition of carbonized PAN/SAN/SWNT composite films determined from XPS

	C (%)	O (%)	N (%)
PAN1–SAN0	86.1	10.0	3.9
PAN1–SAN10	82.1	13.5	4.4
PAN1–SAN30	82.1	15.6	2.3
PAN1–SAN50	90.5	6.6	2.9
PAN2–SAN30	89.2	7.6	3.2
PAN3–SAN30	84.5	10.8	4.6

4. Conclusions

This study shows that SWNT act as a compatabilizer for PAN/SAN blends. This effect has been used to develop porosity control in the carbonized PAN/SAN/SWNT composites with an average pore size in the range of 3–13 nm. Isothermal N_2 adsorption studies indicate that the pore size depends on SAN copolymer content as well as on the SWNT:PAN ratio. Extremely high electrical double layer capacity in the range of 83–205 μF/cm^2 has been observed in the ternary composites. By comparison, the double layer capacity for various carbon materials reported in the literature to date is in the range of 3–70 μF/cm^2. The high double layer capacity values obtained for the PAN/SAN/SWNT ternary composite point to the potential of this approach for developing extremely high charge storage capacity carbon electrodes.

Acknowledgement

This work is supported by AFOSR (F49620-03-1-0124 and FA9550-06-1-0315), ONR (N00014-03-1-0688), and Carbon Nanotechnologies Inc. Useful discussions with Professor Larry Bottomley are gratefully acknowledged.

References

[1] Kinoshita K. Carbon electrochemical and physicochemical properties. New York: John Wiley & Sons; 1988.
[2] Shi H. Electrochimica Acta 1996;41(10):1633.
[3] Yang KL, Ying TY, Yiacoumi S, Tsouris C, Vittoratos ES. Langmuir 2001;17:1961.
[4] Qu D, Shi H. Journal of Power Sources 1998;74:99–107.
[5] Gardner TH, Berry DA, Lyons KD, Beer SK, Freed AD. Fuel 2002;81:2157–66.
[6] Rodriguez-Reinoso F. Carbon 1998;36:159.
[7] Konieczny K, Klomfas G. Desalination 2002;147:109–16.
[8] Torregrosa R, Martin-Martinez JM. Fuel 1991;70(10):1173.
[9] Fodriguezreinoso F, Molinasabio M. Carbon 1992;30(7):1111.
[10] Laine J, Yunes S. Carbon 1992;30(4):601.
[11] Barby D, Haq Z. European patent. 0060138; 1982.
[12] Edwards CJC, Hitchen DA, Sharples M. US patent. 4775655; 1988.
[13] Pekala RW, Alviso CT, LeMay JD. Journal of Non-Crystalline Solids 1990;125:67.
[14] Hatori H, Yamada Y, Shiraishi M. Carbon 1991;30:303.
[15] Conway BE. Electrochemical supercapacitors, scientific fundamental and technological applications. New York: Plenum Publishers, Kluwer Academic; 1999.

[16] Lee J, Han S, Hyeon T. Journal of Materials Chemistry 2004;14(4):478–86.
[17] Jurewicz K, Vix-Guterl C, Frackowiak E, Saadallah S, Reda M, Parmentier J, et al. Journal of Physics and Chemistry of Solids 2004; 65(2–3):287–93.
[18] Vix-Guterl C, Saadallah S, Jurewicz K, Frackowiak E, Reda M, Parmentier J, et al. Materials Science and Engineering B 2004; B108(1–2):148–55.
[19] Kowalewski T, Tsarevsky NV, Matyjaszewski K. Journal of the American Chemical Society 2002;124:10632.
[20] Kim C, Yang KS. Applied Physics Letters 2003;83(6):1216.
[21] An KH, Jeon KK, Heo JK, Lim SC, Bae DJ, Lee YH. Journal of the Electrochemical Society 2002;149(8):A1058.
[22] Ham HT, Choi YS, Jeong N, Chung IJ. Polymer 2005;46(17):6308.
[23] Zhou CF, Kumar S, Doyle CD, Tour JM. Chemistry of Materials 2005; 17(8):1997.
[24] Chiang IW, Brinson BE, Huang AY, Willis PA, Bronikowski MJ, Margrave JL, et al. Journal of Physical Chemistry B 2001;105:8297.
[25] Webb AP, Orr C. Analytical methods in fine particle technology. Norcross, GA: Micromeritics Instrument Corp.; 1997.
[26] Liu T, Sreekumar TV, Kumar S, Hauge RH, Smalley RE. Carbon 2003;41:2440–2.
[27] The term "bucky paper" is used for a carbon nanotube film.
[28] Albrecht W, Malsch G, Weigel Th, Klug P, Makschin W, Grobe V. Acta Polymerica 1992;43(2):119.
[29] Sreekumar TV, Liu T, Min BG, Guo H, Kumar S, Hauge RH, et al. Advanced Materials 2004;16:58.
[30] Chae HG, Sreekumar TV, Uchida T, Kumar S. Polymer 2005;46: 10925–35.
[31] Barisci JN, Wallace GG, MacFarlane DR, Baughman RH. Electrochemistry Communications 2004;6:22.
[32] Frackowiak E, Beguin F. Carbon 2001;39(6):937–50.
[33] Beguin F, Szostak K, Lota G, Frackowiak E. Advanced Materials 2005; 17:2380.
[34] Chastain J. Handbook of X-ray photoelectron spectroscopy. Eden Prairie, Minnesota: Perkin–Elmer Corporation, Physical Electronics Division, Inc.; 1992. p. 41.
[35] Wang PH, Hong KL, Zhu QR. Journal of Applied Polymer Science 1996;62:1987.